



ELSEVIER

Catena 51 (2003) 33–43

CATENA

www.elsevier.com/locate/catena

Sediment transport in rill flow under deposition and detachment conditions

V.O. Polyakov*, M.A. Nearing

USDA-ARS National Soil Erosion Research Laboratory, West Lafayette, IN 47907-1196, USA

Received 26 July 2001; received in revised form 19 February 2002; accepted 28 June 2002

Abstract

The understanding of soil erosion processes and the development of accurate erosion prediction models require understanding of detachment, deposition, and sediment transport in rills. The objectives of this study were to determine whether sediment transport capacity is a unique value for given soil, flow rate, and slope, and to determine if equilibrium sediment concentration in the rill obtained by detachment was different from that observed under depositional conditions. Experiments on a Carmi loam (fine, mixed, mesic Typic Hapludalf) simulated rill erosion under net detachment and net deposition conditions. Two discharge rates of 6 and 9 l min⁻¹ and two sediment input regimes of 0 and excess of transport capacity were tested on soil beds with lengths of 2, 4, 6, 7, and 8 m at 7% slope. Sediment load reached steady state conditions within the 8-m distance on the rill. At 9 l min⁻¹ discharge, 8 m length, and excess sediment added to the flow, sediment delivery was 71 g l⁻¹ versus 31 g l⁻¹ for the corresponding case with no sediment added. Overall, for the conditions tested, rill flow transported two times more sediment than it could detach. The flow did not reach its maximum potential transported load through detachment of soil due in part to changes in the sediment size distribution under deposition and possibly to the protective action of bedload particles moving along the rill bottom and/or changes in flow turbulence associated with sediment laden flow. © 2003 Elsevier Science B.V. All rights reserved.

Keywords: Erosion; Rill erosion; Runoff; Sediment; Sediment transport; Soil erosion

1. Introduction

Detachment is the dislodging of particles from the soil matrix by erosive agents. This occurs by several processes, predominant of which are the hydraulic forces of raindrop

* Corresponding author.

E-mail address: polyakov@ecn.purdue.edu (V.O. Polyakov).

impact and surface runoff in rills. There are several different conceptual models for soil detachment in rills, including relationships involving flow discharge rate (Meyer and Wischmeier, 1969), hydraulic shear stress (Nearing et al., 1989), and streampower (Nearing et al., 1997).

A common conceptualization of rill detachment is a first-order differential model of the form:

$$dc/dx = \alpha (1 - c/T_c) \quad (1)$$

where x is the distance along the rill bed (m), c is sediment concentration (kg m^{-3}), T_c is the transport capacity of the flow expressed as concentration (kg m^{-3}), and α is an empirical coefficient (Nearing et al., 1990).

Transport capacity is the equilibrium sediment concentration approached at an infinite downslope distance given that hydraulic conditions (discharge, channel roughness, slope) do not change. The solution for Eq. (1) for the case of steady state, uniform flow is:

$$c = T_c(1 - e^{-\beta x}) \quad (2)$$

where β is equal to α/T_c .

A slightly different approach to modeling rill erosion does not use an explicit calculation of sediment transport capacity, but rather tracks sediment concentration as a balance of instantaneous detachment and deposition rates along the rill bed (Rose et al., 1983; Hairsine and Rose, 1992a,b). In this case, soil detachment rate is assumed to be limited by the deposited sediment on the rill bed, which acts to protect the rill bed from detachment forces of the flow. Since the amount of sediment on the rill bed at a given time is a first-order function of the amount of sediment in the flow, and since the detachment rate is a first-order function of the bed cover, the result for uniform, steady state flow is a first-order relationship between detachment and sediment concentration essentially similar in solution to Eq. (2) above.

When sediment load exceeds sediment transport capacity, deposition occurs. Net deposition is calculated from equation (Nearing et al., 1990):

$$D_f = (V_f/q) (T_c - G) \quad (3)$$

where V_f is effective fall velocity of the detached sediment (m s^{-1}), q is runoff rate per unit width ($\text{m}^2 \text{s}^{-1}$), T_c is sediment transport capacity ($\text{kg s}^{-1} \text{m}^{-1}$), and G is sediment load ($\text{kg s}^{-1} \text{m}^{-1}$).

In general, transport capacity is a function of the flow's hydraulic forces and the transportability of the sediment. Usually, transport capacity of rill flow is estimated using some combination of total flow discharge rate, flow width, velocity, slope, sediment characteristics, and rill geometry. Nearing et al. (1997) tested several different hydraulic parameters and found streampower best related to sediment load for a very wide range of hydraulic and material conditions, including cohesive soil. Using data from 400 experiments with well-sorted granular quartz, Govers (1990) concluded that the transport capacity of overland flow was best related to grain size and either fluid shear stress or unit streampower.

In both of the above cases, the experimental method for measuring “transport capacity” involved placing material along the flume bed and introducing clear water at the upstream end. In both cases, the bed was clearly long enough for length equilibrium to be established, and the resultant sediment load was considered to be the transport capacity. Certainly, in the landscape, a correspondent condition can and will arise on portions of hillslopes where detachment takes place, such as the upper and middle sections of a hill. However, on the lower end of the hillslope, as the slope decreases, or on the entirety of the hillslope during the recession phase of a storm, the situation is much different. In this case, the sediment is carried in the flow from upstream sources, and the question is how much the flow will continue to move downslope. In erosion models, these two cases are treated essentially the same. A single functional relationship for transport capacity is used in both cases. In other words, for the same sediment material, hydraulic conditions, and slope, transport capacity is calculated as the same value regardless if approached from the detachment or depositional side.

The objective of this study was to test the implicit assumption of erosion models that sediment transport capacity is a unique value for given soil type, flow rate, and slope. In other words, we sought to determine if the sediment concentration in the flow obtained from distance equilibrium under detachment conditions was different from that obtained from equilibrium depositional conditions.

2. Methods

The soil used in the study was a Carmi loam (fine, mixed, mesic Typic Hapludalf) with 15% clay, 58% silt, and 27% sand content. The soil was formed in late-Wisconsinan loess, and is dark colored, deep, and well drained with rapid permeability.

The soil was air dried and passed through an 8-mm sieve. An 8-m long and 61-cm wide hydraulic flume was used. The depth of soil in the flume was approximately 15 cm. The flume slope was adjusted to 7%. Water was supplied to the upper end of the rill via an aluminum tray, which could be set at different points along the slope in order to create varied lengths of the rill. A sediment feeder was used to supply dry soil material as sediment into the flow at controlled rates. The sediment feeder could be moved along the rill to direct the input sediment to the tray where it mixed with the inflow of clean flowing water.

Prior to the run, the soil surface was formed into a slight V-shape with approximately 2% side slopes. Before runs, the soil was allowed to wet slowly to saturation for 24 h, with the flume in a horizontal position. Preparation for consecutive runs included drying, replacing top layer of soil and material lost from the prior experiments with new sieved soil, breaking up clods, and smoothing out irregularities on the surface.

Independent variables in this study were flow rate, rill length, and added sediment load. Levels of independent variables in this study were: water inflow rates of 6 and 9 l/min; rill lengths of 2, 4, 6, 7, and 8 m; sediment feeder discharges of 0 and 620 g/min (for the 6-l/min flow), and 0 and 1500 g/min (for the 9-l/min flow). Slope was 7% for all runs. Each experimental treatment was replicated.

The experiments were designed to provide data on transport capacity of rill flow both with additional sediment input (i.e., under active, net deposition) and without additional

sediment input (i.e., with active, net detachment). In order to quantify sediment load for the two different conditions, each run was divided into six periods. The purpose of periods 1, 3, and 5 was to find the equilibrium conditions for sediment concentration when no extra sediment is added to the flow. The purpose of periods 2, 4, and 6 was to find equilibrium with additional sediment input. During the first period, clean water was supplied to the top of the rill. During the second period, the rill was supplied with a water and sediment mixture. The amount of sediment added was greater than transport capacity of the flow and varied depending on flow discharge (see treatment levels above). These levels were determined from preliminary testing of the system (data not reported). Alternating between periods of no-sediment inflow with sediment loaded inflow made it possible to bring the sediment concentration to temporal equilibrium three times from the deposition side and three times from the detachment side. When the sediment concentration curve (Fig. 1) became horizontal, it was considered that time equilibrium had been reached after the abrupt shift to the deposition or detachment regimes. Thus, only the last 10 samples (out of the total 15) in each period of the run were used to calculate equilibrium sediment load. A total of 1200 data points for sediment concentration were used in the analysis.

Sediment was added as a continuous feed of dry soil material. The dry sediment was added onto a submerged metal plate just above the entrance of the flow into the rill, where it was wet and mixed with water. This prevented hydrophobicity and air-trapping effects, and helped sediment to enter the flow.

Testing of the various rill lengths allowed quantification of sediment load as a function of distance. Experiments lasted from 45 to 180 min, depending on the length of the rill and the discharge rate. Velocity was measured by injecting dye at a point and recording the time required for the leading edge of the dye to travel 2 m. Velocity for the 8-m rill was

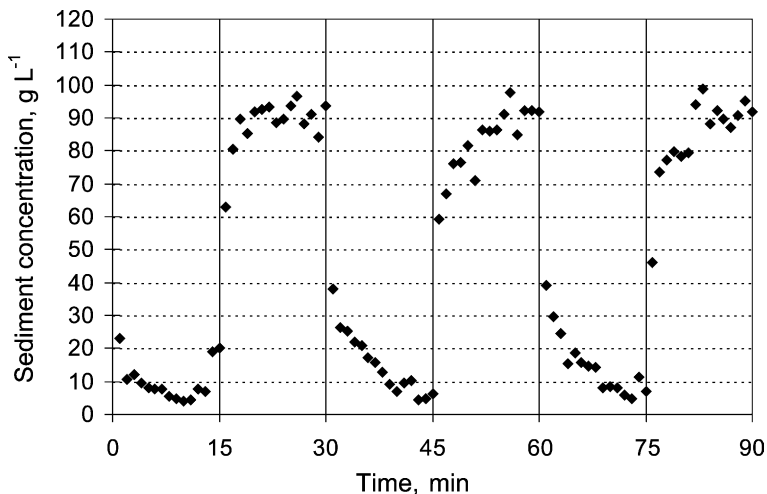


Fig. 1. Sediment concentrations as a function of time during the experiment for the case of the 2-m rill at a flow rate of 6 l min^{-1} . Periods 1, 3, and 5 represent the case of no sediment added and periods 2, 4, and 6 represent the case of excess sediment added to the upper end of the rill.

measured at 0–2, 2–4, 4–6, and 6–8 m, then averaged to obtain the value for the entire rill. Velocity for the 6-m rill was measured at 0–2, 2–4, and 4–6 m. Velocity for the 4-m rill was measured at 0–2 and 2–4 m. Velocity of the 2-m rill was measured over the 2-m length of the rill. Velocity of the leading edge of fluorescent dye was adjusted to average flow velocity with the correction factor of 0.57 (Gilley et al., 1990).

Width of the flow was measured with a ruler at each 0.5 m along the rill. The channel was assumed to be rectangular for purposes of flow depth calculations. Thus, depth, H (m) was calculated as:

$$H = Q/(wv) \quad (4)$$

where Q ($\text{m}^3 \text{s}^{-1}$) is total discharge, w (m) is average flow width, and v (m s^{-1}) is the measured velocity.

In any erosion experiment involving rills, it is important to characterize the flow regime in order to put the results into context. This is particularly true when other workers want to compare the results of previous experiments. Thus, we calculated the nondimensional Reynold's and Froude numbers for these experiments. Reynold's number is calculated as the ratio of flow velocity multiplied by hydraulic radius to the kinematic viscosity of water. It is essentially a ratio of kinetic to viscous forces of the flow. Froude number is the ratio of flow velocity to the square root of the quantity of flow depth multiplied by the gravitational constant. It represents a ratio of kinetic to gravitational flow forces.

The aggregate stability and size distribution measurements (Kemper and Rosenau, 1986) were made with a slightly modified method to fit the circumstances. Because we studied aggregates in runoff, collected samples were neither air dried nor sieved through a 2-mm sieve prior to analysis, as recommended by the standard method. Laboratory analyses were performed immediately after samples of runoff were collected.

3. Results and discussion

Froude and Reynold's numbers observed in these experiments were within the range reported for rills by Nearing et al. (1997). The Reynold's number ranged between 400 and 1500 and Froude number varied from 0.25 to 2.1. Most of the data represent supercritical turbulent hydraulic regime, though for the 6-l-min^{-1} discharge rate when sediment was not added, the data fell mostly in the subcritical turbulent regime.

Fig. 1 shows a typical result of the experiments, in this case for the 6-l-min^{-1} flow rate and rill length of 2 m. The times from 0 to 15, 30 to 45, and 60 to 75 min represent periods of no added sediment. The gradual reduction in sediment in the third and fifth periods represents the system approaching temporal equilibrium. The times from 15 to 30, 45 to 60, and 75 to 90 min represent periods of added sediment, in this case at a rate of 620 g min^{-1} . Note that for the 6-l-min^{-1} flow rate, the addition of 620 g min^{-1} represents an effective concentration of 103 g l^{-1} , which is greater than the concentration of sediment leaving the flume (Fig. 1). In other words, the system experienced net deposition in periods 2, 4, and 6. In all cases, the experimental run times were long enough so that temporal equilibrium of the system was obtained.

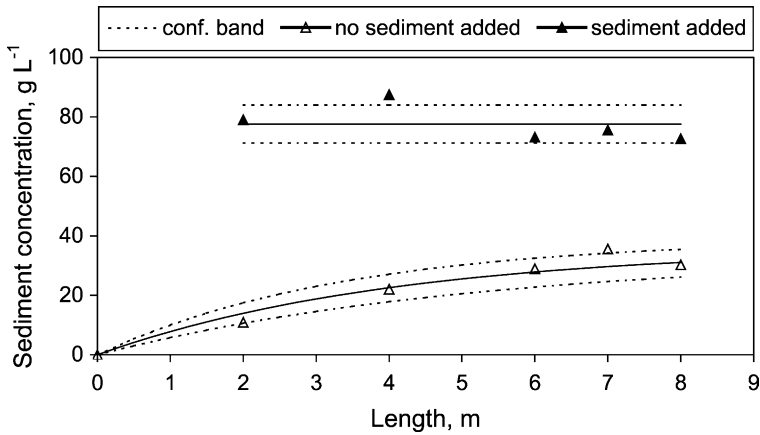


Fig. 2. Average time equilibrium sediment concentrations as a function of rill length for the cases of sediment added and no sediment added at 6 l min⁻¹ flow discharge rate.

Figs. 2 and 3 show equilibrium sediment concentration as a function of rill length. For the detachment case (corresponding to time equilibrium sediment concentrations from periods 1, 3, and 5 from both replicates), the data were consistent with the first order detachment model (Eqs. (1) and (2)). For the 6-l-min⁻¹ case, Eq. (2) may be written as

$$c = 36.2(1 - e^{-0.243x}) \quad (r^2 = 0.93) \tag{5}$$

and for the 9-l-min⁻¹ case, Eq. (2) may be written as

$$c = 54.4(1 - e^{-0.364x}) \quad (r^2 = 0.68) \tag{6}$$

where c is in units of g l⁻¹. This means that for 6 and 9 l min⁻¹, treatments transport capacity was 36.2 and 54.4 g l⁻¹, respectively.

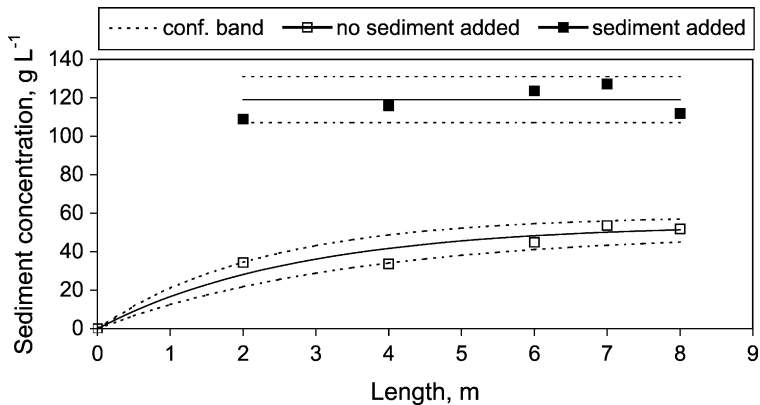


Fig. 3. Average time equilibrium sediment concentrations as a function of rill length for the cases of sediment added and no sediment added at 9 l min⁻¹ flow discharge rate.

For the case where sediment was added to the top of the rill (corresponding to time equilibrium sediment concentrations from periods 2, 4, and 6 from both replicates), the rill length had no significant influence on sediment concentration. This leads to the conclusion that under these conditions with no change in bed slope, sediment deposited very quickly (prior to the 2-m distance) and the concentration of sediment from that point on was essentially constant. The sediment discharge from the flume when sediment was added to the flow was $77.6 \pm 6.4 \text{ g l}^{-1}$ ($\alpha=0.05$) for the 6-l-min^{-1} flow rate, and $119.1 \pm 12.0 \text{ g l}^{-1}$ for the 9-l-min^{-1} flow rate. Thus, the equilibrium sediment concentration was 2.1 and 2.2 times greater for the case of added sediment compared to the case of no added sediment for the 6- and 9-l-min^{-1} flow rates, respectively.

These results show that equilibrium sediment concentration relative to rill length was met or closely approached in these experiments. Detachment-limiting and transport-limiting curves for each of the discharges did not converge and their confidence bands did not overlap (Figs. 2 and 3). This means that equilibrium conditions for two regimes are statistically different.

Our experiment indicates a hysteresis phenomenon in the sediment transport relationship. Equilibrium maximum concentration of sediment differs depending upon whether it is approached from sediment excess or sediment deficit. Hysteresis is a characteristic feature of many natural systems. When a system is disturbed in different ways, it does not necessarily follow the same path to return to equilibrium, or it may not return to the same state of equilibrium at all. This study illustrates the hysteresis concept through observations of the erosion process. Irrespective of the cause of this phenomenon, this result has major implications for erosion modeling. A factor of 2 in the difference between “sediment transport capacities” when in the net depositional phase as compared to the net detachment phase represents a major factor for which to be accounted.

We hypothesize and discuss here four possible physical explanations for this large discrepancy in the equilibrium sediment concentration under the two sediment regimes of detachment and deposition: (1) sediment size differences due to preferential deposition of coarse sediment in the flow and/or rapid wetting of the introduced dry sediment, (2) changes in hydraulic friction due to a smoothing of the soil bed under the deposition regime, (3) physical protection from detachment of soil from the rill bottom by moving bedload, or (4) significantly less energy required to maintain the movement of the sediment in the flow compared to that required to detach new material from the soil bed. The sieve analysis of the aggregates indicated a clear difference in the size of the sediment for the case where no sediment was added compared to the case with sediment added (Table 1). The percentage of coarse particles in sediment was reduced and the percentage of fine particles was increased when sediment was added to the flow. However, even though the percentage of coarse sediment was less for the sediment-added case, the actual mass load of the coarse particles, and indeed of all of the sediment size classes, was still greater when sediment load was added as compared to the no-sediment-added case (see columns 6 and 7, Table 1). Due to experimental method used, added sediments were air dried when introduced into the flow. This, probably, have caused flaking due to rapid wetting and, as a consequence, reduction in aggregate size. It certainly complicates the comparison of sediment aggregate sizes between two regimes. Despite the fact that flaking occurred, the mass of any given sediment size class during net deposition regime was

Table 1
Size distribution and sediment load by size class of eroded aggregates

Discharge ($l\ min^{-1}$)	Rill length (m)	Sieve size (mm)	Aggregate fraction retained (%)		Sediment concentration of each aggregate fraction ($g\ l^{-1}$)	
			No Sediment added	Sediment added	No sediment added	Sediment added
6	2	4.76	3	1	0.3	0.8
		2	18	9	2.0	7.1
		1	21	9	2.3	7.1
		0.21	26	20	2.8	15.8
		<0.21	32	61	3.5	48.2
	8	4.76	2	2	0.6	1.5
		2	15	10	4.5	7.3
		1	19	14	5.7	10.2
		0.21	21	24	6.4	17.4
		<0.21	43	51	13.0	37.0
9	2	4.76	4	3	1.4	3.3
		2	17	9	5.9	9.8
		1	17	8	5.9	8.7
		0.21	23	20	7.9	21.8
		<0.21	39	61	13.4	66.5
	8	4.76	4	2	2.1	2.2
		2	21	10	10.9	11.2
		1	20	16	10.4	17.9
		0.21	24	27	12.4	30.2
		<0.21	30	44	15.5	49.2

greater than corresponding class during net detachment regime. Aggregate breakdown along with sediment sorting, which occurred with deposition, may explain a portion, but not all of the difference in the observed equilibrium sediment loads between the cases of sediment added vs. no sediment added.

The second possible explanation for the large differences in equilibrium sediment load between the detachment and deposition cases is related to differences in hydraulic roughness. This reasoning relates to the fact that rough surfaces act to dissipate a portion of the flow energy, thus making it unavailable for sediment transport. The average Darcy–Weisbach friction factors were, on average, lower (Fig. 4) for the case of added sediment as compared to no added sediment. There was no apparent trend in the friction factor as a function of sediment load within the sediment-added case (Fig. 4), which would indicate that these rills have reached a smooth state due to the deposition incurred. What is perhaps more interesting is that for the higher sediment concentrations of the no-sediment-added case, the friction factors were essentially the same as for the sediment-added case (Fig. 4). This was true even though total sediment concentrations were much less for the no-sediment-added case at the corresponding rill lengths (Table 2). This result suggests that the differences in the hydraulic friction of the rill beds also do not explain all the observed differences in the equilibrium (with rill length) sediment concentrations between the two

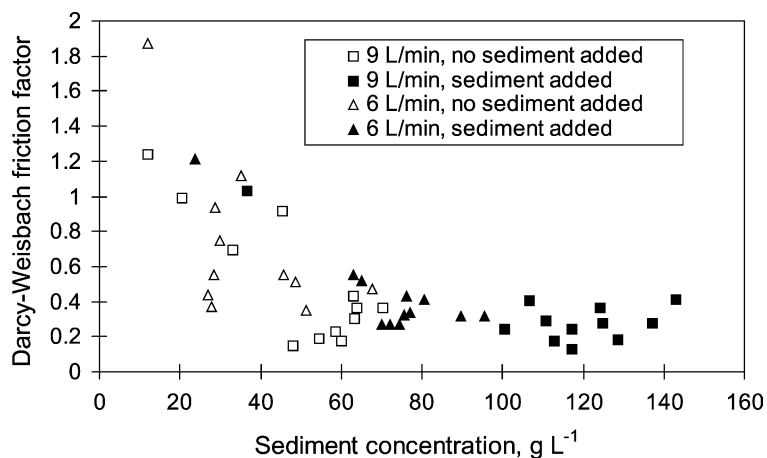


Fig. 4. Darcy–Weisbach hydraulic friction factor as a function of sediment concentration for the cases of sediment added and no sediment added at both 6 and 9 l min^{-1} flow discharge rates.

cases. Another point which is of interest here is that equilibrium sediment concentrations were greater for the sediment-added case in spite of the fact that flow was wider and flow depths were shallower for the sediment-added case, which implies lower surface shear

Table 2

Mean sediment concentrations, flow width, and flow depth for the two sediment transport regimes: (a) no sediment added to the upper end of the rill and (b) sediment added to the upper end of the rill

Discharge (l min^{-1})	Transport regime	Rill length (m)	Sediment concentration (g l^{-1})	Flow width (cm)	Flow depth (cm)		
6	no sediment added	2	10.94	7.9	0.66		
		4	22.06	7.8	0.61		
		6	28.90	8.1	0.56		
		7	35.56	8.5	0.57		
	sediment added	8	30.25	10.1	0.51		
		2	78.98	9.5	0.45		
		4	87.51	10.5	0.39		
		6	73.16	9.4	0.45		
		7	75.58	10.1	0.40		
		8	72.63	10.5	0.40		
		9	no sediment added	2	34.42	10.9	0.54
				4	33.72	10.0	0.63
6	44.92			7.6	0.78		
7	53.59			11.7	0.49		
sediment added	8		51.8	12.2	0.57		
	2		109.00	13.2	0.42		
	4		115.91	12.4	0.47		
	6		123.69	9.3	0.59		
		7	127.24	13.2	0.43		
		8	111.85	14.2	0.43		

stresses for this case as compared to the no-sediment-added case (Table 2). Based on these arguments, we conclude that differences in flow hydraulics did not contribute greatly to the observed differences in equilibrium sediment loads between the sediment-added case vs. the no-sediment-added case.

Given that differences in flow hydraulics do not explain the difference between sediment loads under the sediment-added vs. the no-sediment-added treatments, and that sediment size differences account for only a portion of the observed sediment load differences, it may be that the observed differences were due in part or largely to the shielding of the soil surface by sediment particles in the flow which prevent further detachment of soil and/or simply that less energy is required to move sediment than to detach soil. This second point may be related to turbulence. Turbulence is essential for soil detachment to occur (Nearing et al., 1991; Nearing, 1991; Nearing and Parker, 1994), and we know that turbulent intensity is less for flows that contain greater sediment loads (Einstein and Chien, 1954; Vanoni and Namicos, 1960; Wijetunge and Sleath, 1998), although recent evidence suggests that such an effect is not present in all cases (Mendoza and Zhou, 1997; Lyn, 1992). A recent rill erosion study (Merten and Nearing, 2001) suggests that reduction of turbulence and protection of the soil by bedload both contribute to the limit imposed on sediment loads in the detachment phase of rill erosion. What may have occurred in the current study was that with the reduction in turbulence associated with increasing sediment in the flow, detachment rates were increasingly limited, while continued downstream movement of sediment in the flow was not hindered by the reduction of turbulence. Visual observation of the sediment in the rill suggests that the bedload moves in the shallow flow by rolling along the bed, a process that, in either turbulent or laminar flow, is facilitated by the greater flow velocity at the top of the rolling aggregate compared to the flow velocity near the bed surface.

The potential mechanisms discussed above for the phenomenon observed in these experiments are not proven by the experiment. More work is necessary to understand the intricate roles and interactions of turbulence, shielding of the soil bed by bedload, the processes of bedload transport in very shallow flows, and the amount of sediment being transported which affect rill erosion.

Regardless of the processes involved, however, the major differences shown in this experiment between equilibrium sediment loads in the detachment regime and equilibrium conditions in the depositional regime should be addressed in erosion models. Some process-based models, such as the WEPP model (Nearing et al., 1989), do account for changes in transport capacity caused by sediment sorting with deposition. But the current study suggests that this is not the only, nor even the primary, mechanism to account for the large observed differences in sediment load for the two cases. WEPP and other process-based models should be modified to account for this fact.

While recognizing that transport capacity generally refers to the value to which sediment concentrations approach at an infinite downslope distance given that discharge and channel slope do not change, the term needs to be further clarified. Transport capacity implies uniqueness, but as was shown here, sediment load equilibrium is not a unique value, but rather a hysteresis phenomenon that depends on the sediment regime.

References

- Einstein, H.A., Chien, N., 1954. Second Approximation To The Solution Of The Suspended Load Theory. Fluid Mechanics Laboratory, University of California, Berkeley.
- Gilley, J.E., Kottwitz, E.R., Simanton, J.R., 1990. Hydraulic characteristics of rills. *Trans. ASAE* 33, 1900–1906.
- Govers, G., 1990. Empirical relationship for the transporting capacity of overland flow. In: Walling, D.E., Yair, A., Berckowicz, C. (Eds.), *Erosion, Transport, and Deposition Processes*. Proceedings of the Jerusalem Workshop, vol. 189. IAHS Pub., Wallingford, UK, pp. 45–64.
- Hairsine, P.B., Rose, C.W., 1992a. Modeling water erosion due to overland flow using physical principles: 1. Sheet flow. *Water Resour. Res.* 28, 237–243.
- Hairsine, P.B., Rose, C.W., 1992b. Modeling water erosion due to overland flow using physical principles: 2. Rill flow. *Water Resour. Res.* 28, 245–250.
- Kemper, W.D., Rosenau, R.C., 1986. Aggregate stability and size distribution. In: Klute, A. (Ed.), *Methods of Soil Analysis*. ASA, Madison, WI, pp. 425–442.
- Lyn, D.A., 1992. Turbulence characteristics of sediment-laden flows in open channels. *J. Hydraul. Eng.* 118 (7), 971–988.
- Mendoza, C., Zhou, D.H., 1997. Energetics of sediment-laden streamflows. *Water Resour. Res.* 33 (1), 227–234.
- Merten, G.H., Nearing, M.A., 2001. Effect of sediment load on soil detachment and deposition in rills. *Soil Sci. Soc. Am. J.* 65, 861–868.
- Meyer, L.D., Wischmeier, W.H., 1969. Mathematical simulation of the process of soil erosion by water. *Trans. ASAE* 12 (6) 754–758, 762.
- Nearing, M.A., 1991. A probabilistic model of soil detachment by shallow turbulent flow. *Trans. ASAE* 34, 81–85.
- Nearing, M.A., Parker, S.C., 1994. Detachment of soil by flowing water under turbulent and laminar conditions. *Soil Sci. Soc. Am. J.* 58, 1612–1614.
- Nearing, M.A., Foster, G.R., Lane, L.J., Finkner, S.C., 1989. A process based soil erosion model for USDA water erosion prediction project technology. *Trans. ASAE* 32, 1587–1593.
- Nearing, M.A., Lane, L.J., Alberts, E.E., Laflen, J.M., 1990. Prediction technology for soil erosion by water: status and research needs. *Soil Sci. Soc. Am. J.* 54, 1702–1711.
- Nearing, M.A., Bradford, J.M., Parker, S.C., 1991. Soil detachment by shallow surface flow at low slopes. *Soil Sci. Soc. Am. J.* 55, 339–344.
- Nearing, M.A., Norton, L.D., Bulgakov, D.A., Larionov, G.A., West, L.T., Dontsova, K.M., 1997. Hydraulics and erosion in eroding rills. *Water Resour. Res.* 33 (4), 865–876.
- Rose, C.W., Williams, J.R., Sander, G.C., Barry, D.A., 1983. A mathematical model of soil erosion and deposition processes: II. Application to data from an arid-zone catchment. *Soil Sci. Soc. Am. J.* 47, 996–1000.
- Vanoni, V., Namicos, G.N., 1960. Resistance properties of sediment-laden strains. *Trans. ASCE* 125, 30–55.
- Wijetunge, J.J., Sleath, J.F.A., 1998. Effects of sediment transport on bed friction and turbulence. *J. Waterw. Port Coast. Ocean Eng.* 124, 172–178.